Journal of Microscopy, Vol. 194, Pt 2/3, May/June 1999, pp. 537–541.
Received 6 December 1998; accepted 9 February 1999

Near-field optical photomask repair with a femtosecond laser

K. LIEBERMAN, Y. SHANI, I. MELNIK, S. YOFFE & Y. SHARON
Nanonics Lithography Ltd, The Manhat Technology Park, Malcha, Jerusalem 91487, Israel

Key words. Laser ablation, near-field optics, photomask repair.

Summary

We present a high-resolution near-field optical tool designed for repair of opaque defects in binary photomasks. Both instrument design and near-field imaging and patterning results will be presented. Designed for ablative processing of thin metal films, the MR-100 incorporates an industrial amplified femtosecond laser, third harmonic generator and built-in autocorrelator. The ultrashort duration of the femtosecond pulses enables the tool to remove chrome layers with negligible damage to the surrounding metal or the underlying quartz substrate. The micropipette based near-field writing head can deliver power densities of hundreds of GW/cm^2 to spots of several hundred nanometres and below. Repairs on sample masks will be presented and the repair quality will be discussed.

Introduction

The capabilities of existing mask repair tools are not sufficient to meet the requirements of the next generation masks that are scheduled to be introduced within two years for the 0·13 μm lithography requirements (International Sematech Lithography Road Map, 1998). Current optical repair tools do not have the imaging resolution or optical placement accuracy to meet the required edge placement tolerances. Focused ion beam (FIB) techniques on the other hand, are capable of very high resolution but are limited by the damage that the ion beam causes to the quartz substrate of the photomask. This ion staining is becoming more severe as the lithography wavelengths move further into the UV. The tool described in this paper achieves repair resolutions comparable to those of FIB machines while providing superior surface restoration properties due to its purely optical material interaction. The combination of imaging and then ablating with the same micropipette allows overall edge placements of better than 50 nm to be achieved.

Correspondence to: K. Lieberman. Tel: + 972 2 679 6601; fax: + 972 2 679 6597; e-mail: klony@netvision.net.il

System description

The basic design on the system is shown schematically in Fig. 1. A straight, hollow metallised micropipette is used as the near-field aperture for both imaging and patterning. Micropipettes, rather than optical fibres, are employed since only micropipettes have the ability to collimate sufficient power to evaporate metal films without themselves being damaged. Details of micropipette manufacture and applications to ablative processing with excimer lasers can be found elsewhere (Rudman *et al.*, 1994; Lieberman *et al.*, 1996). A standard shear-force AFM feedback is employed to track the tip over the surface. A CW doubled Nd:YAG laser is fed into the micropipette for NSOM imaging. The scanning is performed by a hollow compound flexure stage with 2 μm absolute accuracy over an 8 inch travel and 20 nm repeatability over a 50 μm scan field. Apertures on the order of 400 nm are used for this work. While this may seem somewhat large for a near-field aperture, effective, well-defined spot sizes of this magnitude cannot be achieved with far-field optics. Currently, direct processing of metal films at such dimensions is only possible with focused ion beam technology.

The repair process comprises the following steps. First, a transmission near-field image of the defect and surrounding area is obtained. This image is acquired in constant height imaging mode so that there will be no chance of topography coupled artefacts interfering with the near-field image. The operator then marks the area that needs to be removed and the edge of interest to be accurately reconstructed and the computer determines the precise contours of the defect and determines the exposure parameters. The area is then rescanned whilst the ablation laser is fired and the chrome is removed. A post-repair NSOM scan of the same area is then performed to verify the repair.

Femtosecond laser ablation

Previous implementation of the tool incorporated an ArF excimer laser as the ablation source (Lieberman *et al.*,

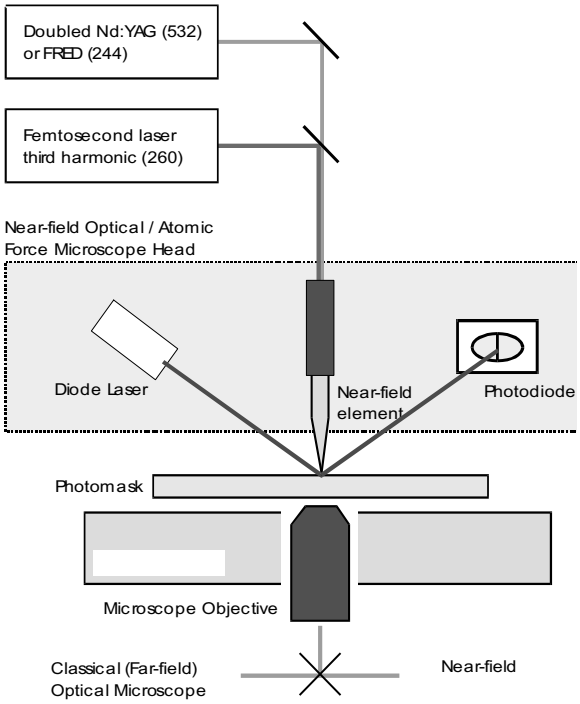

Fig. 1. Schematic layout of the MR-100 near-field system.

1996; Rudman *et al.*, 1994). This laser suffered from several inherent drawbacks that severely hindered the performance. The primary issue related to the relatively long pulse width of $\approx 2{\cdot}5$ ns. Although this is considered to be extremely short for ordinary laser machining processes, due to the

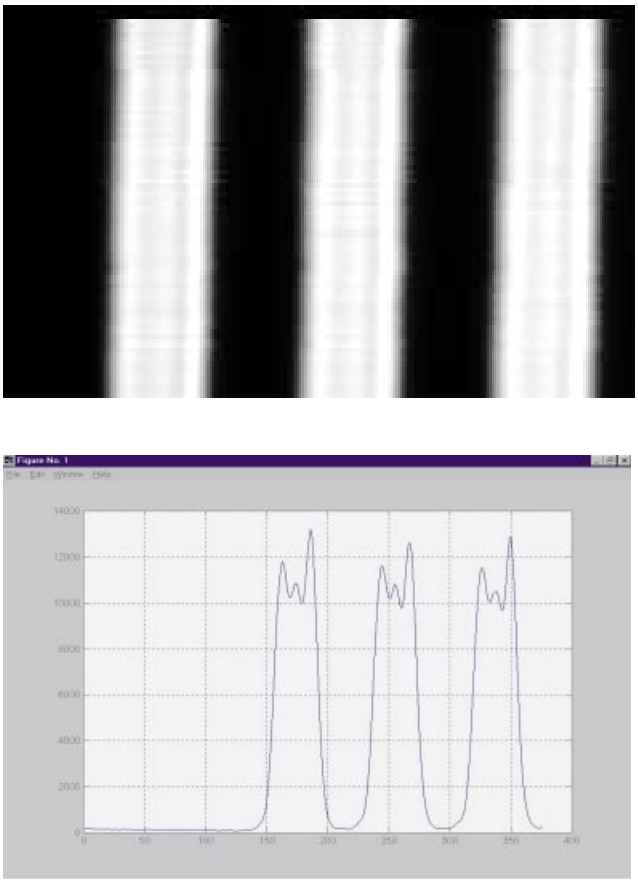

Fig. 3. (A) Constant height NSOM image of a 2 μm period grating. (B) Cross-section line scan extracted from (A).

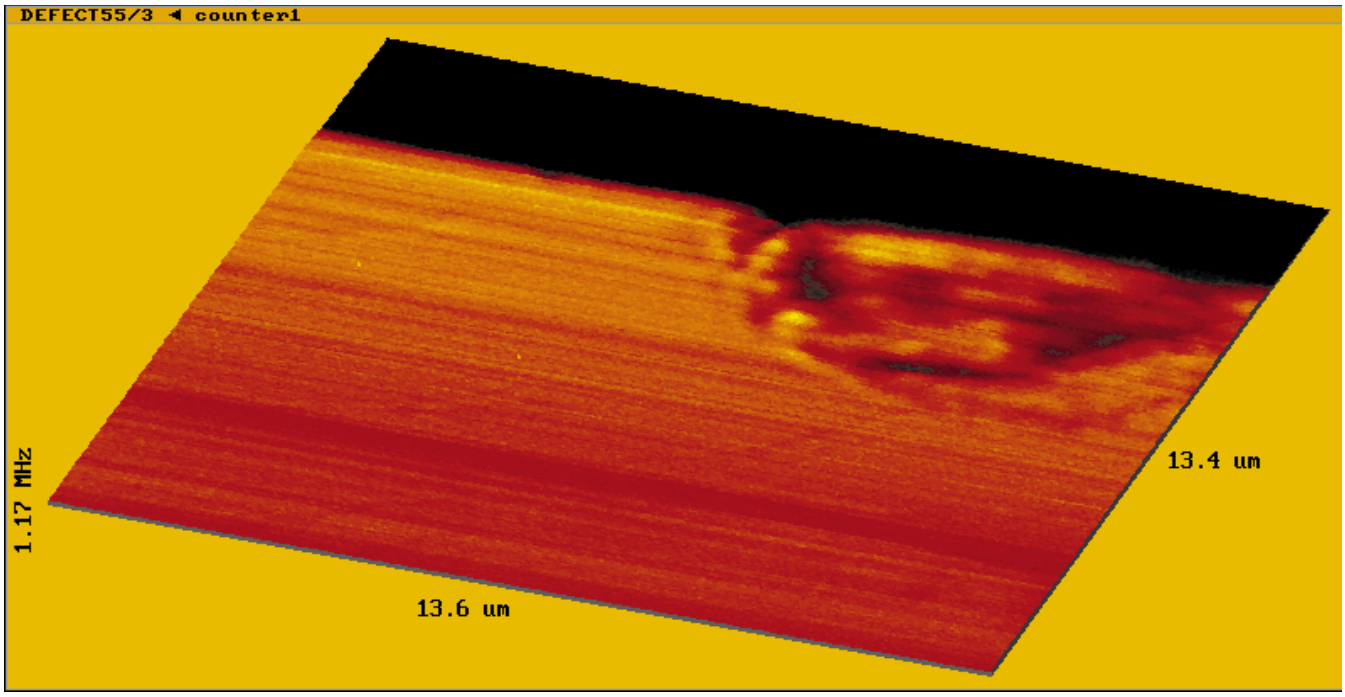

Fig. 2. (A) AFM and (B) transmission NSOM of a chrome defect ablated with an ArF excimer laser.

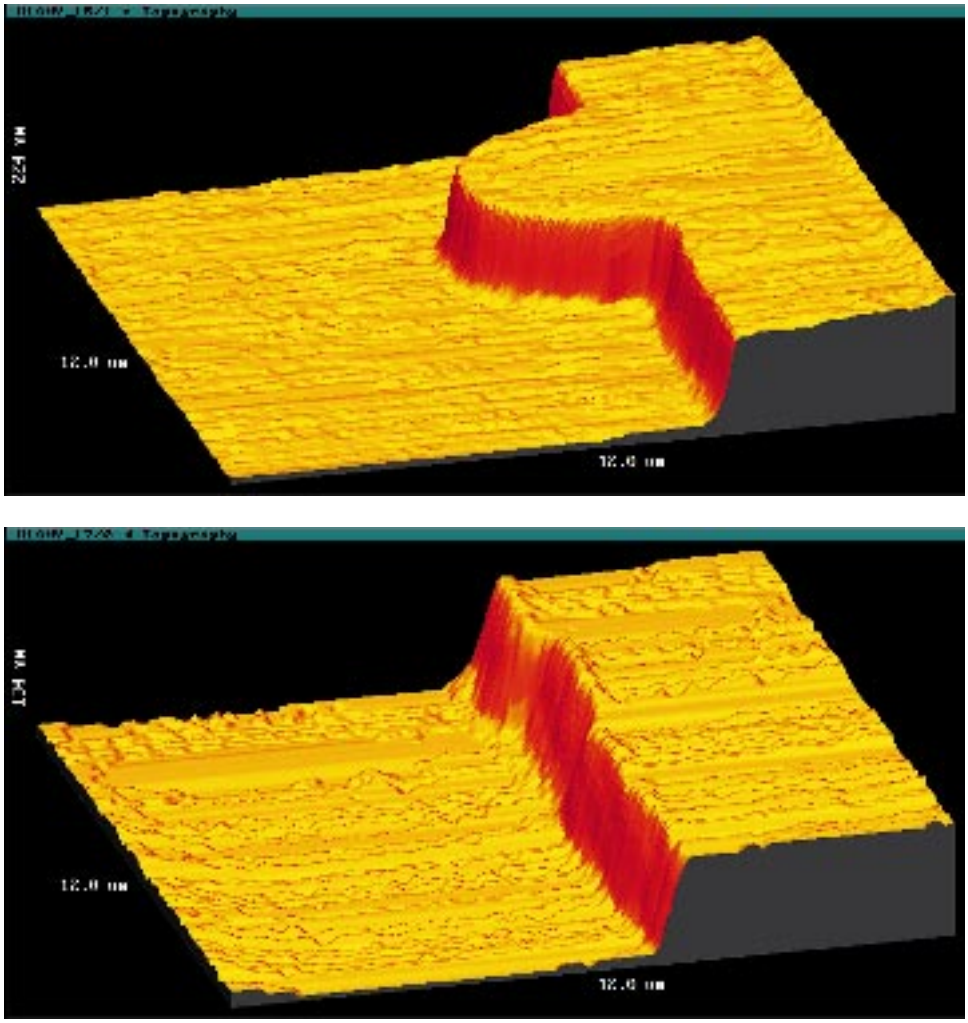

Fig. 4. (A) AFM image of a programmed defect prior to repair. (B) AFM image of the same region after repair.

very high resolutions required by this work, thermal diffusion during the pulse spreads the heat to a region of extending hundreds of nanometres in all directions. Thus, the heat distribution is very uneven, with the centre of the region being heated to evaporation while surrounding areas are melted but not evaporated. Further out the heat causes phase transitions in the metal and accelerates diffusion processes between the chrome and glass interface layer. The result of this is a rather chaotic process that is not easily controlled. It turned out that it was impossible to effectively remove the 100 nm thick chrome layer on the mask without significantly penetrating the quartz substrate. An example of such a process is shown in Fig. 2. The AFM image shows the deep cratering of the substrate, while the transmission NSOM clearly indicates the transmission losses in the processed region, making this repair unacceptable.

The introduction of a femtosecond duration pulsed laser has resolved this issue. With sufficiently short pulses (where the pulse duration is less than the phonon lattice coupling constant) the light which is absorbed by the electrons will ablate the metal, and take the energy with it, before the heat can transfer to the surrounding regions. The mechanics of such ablative removal of metal films with ultrashort pulses has been fairly well characterized (Nolte *et al.*, 1997). Until quite recently however, there were no femtosecond laser systems that were sufficiently reliable to be considered for industrial equipment. The laser we have incorporated, with a fully self-contained fibre oscillator, pump laser, TiS amplifier and pulse compressor, is in a thermally stabilized metal casting. Energy densities on the order of several hundred millijoules/cm^2 can be achieved at the exit aperture of the pipette without damage to the pipette itself.

Edge definition and placement

One of the primary functions of a photomask repair tool is to carve off excess chrome protruding from patterned lines

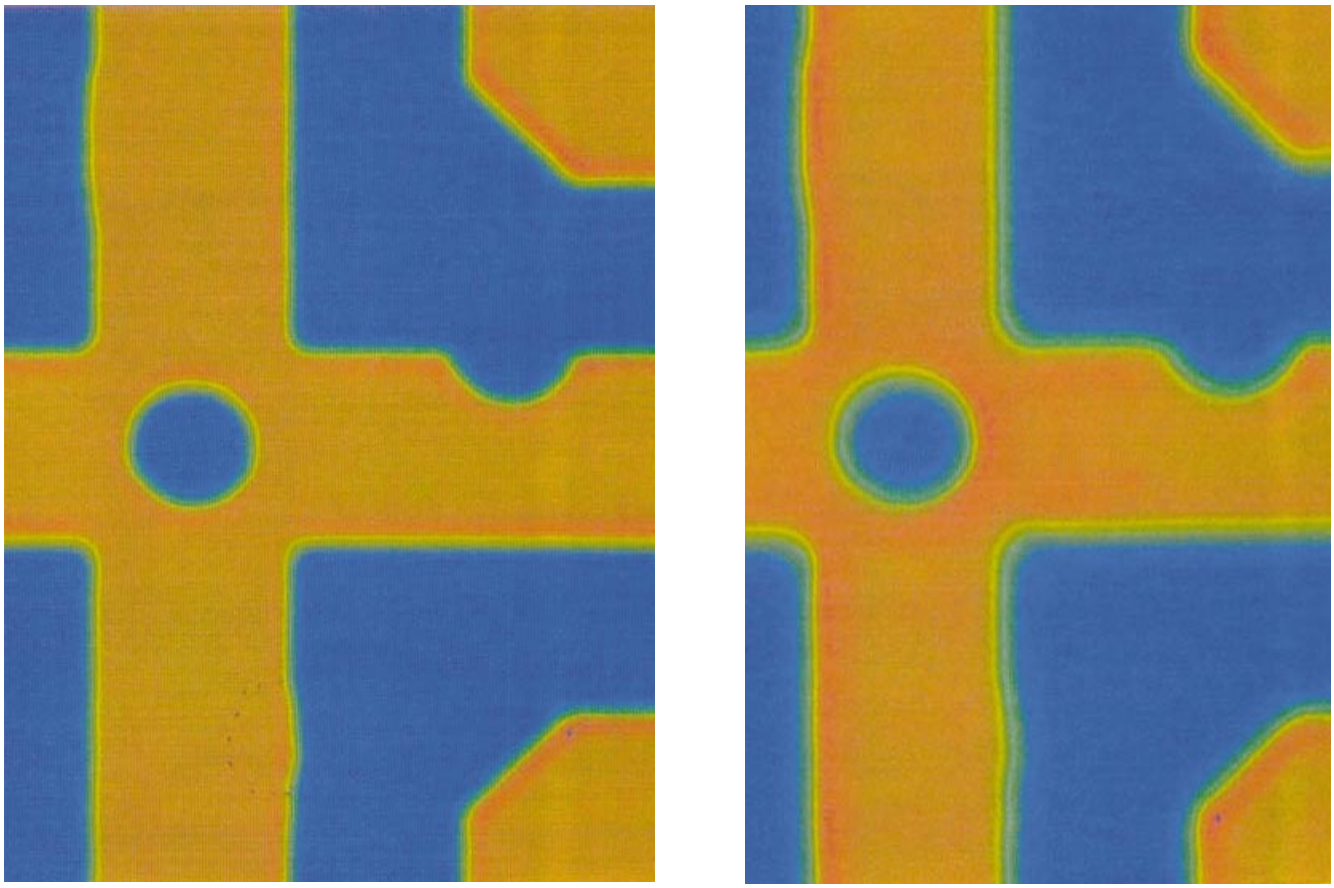

Fig. 5. Arial imaging data (AIMS) at 248 nm of two repaired defects. (A) Image best focus, (B) plus 1 μm defocus.

on the mask. Such protrusions effect the critical dimension (CD) variations on the processed wafer and can significantly impact production yields. Current requirements for the accuracy of edge repairs, as defined by the international SEMATECH organization (Lieberman, 1997) dictate reconstruction of the straight edge to between 30 and 50 nm, depending on the process technology involved. In order to achieve such accuracy it is necessary to determine the position of the edge in the near-field image to a value significantly better than this. Simply choosing the middle, or the maximum gradient of the edge slope in the NSOM image is far from satisfactory, however. As an example see Fig. 3, which is a constant height NSOM image of a 2 μm period grating along with an extracted profile cross-section. Choosing the middle of the rise, even discounting for the spurious polarization-induced edge enhancements visible on either side of the line, gives a consistent placement error of over 100 nm in the direction of the transparent quartz regions. Empirical fitting of these data to the known grating parameters allows us to determine the optimal position with far greater accuracy. In this case, it can clearly be seen that the actual edge is located only at a rise of $\approx$ 35% of the pure quartz transmission value.

Transmission quality after repair

The quality of the exposed quartz after ablative repair is of particular significance to the mask manufacturers. Since current masks operate at a deep ultraviolet illumination wavelength of 248 nm, any residual material, or conversely, any substrate penetration greater than $\approx$ 10 nm, will lead to unacceptable transmission losses or scattering. An example of a high quality repair is seen in Fig. 4. The original programmed defect, a semicircular protrusion in the chrome film 100 nm high can be seen in the AFM image in Fig. 4(A). Another image of the same region after the repair is seen in Fig. 4(B). All the excess chrome has been removed with no damage to the substrate. A slight overcut of $\approx$ 50 nm into the edge can also be seen. Arial imaging measurements (AIMS) of several repaired defect sites can be seen in Fig. 5(A),(B).[1] In these images, which simulate the optical parameters of the steppers used to print the wafers (wavelength, numerical aperture, partial coherence, etc.), it can be seen that there is no loss of transmission throughout the repaired area. In Fig. 5(B) it can be seen that even with 1 μm defocus of the imaging lens the repaired area remains

[1] AIMS images courtesy of Photronics Inc., Milpitas, CA

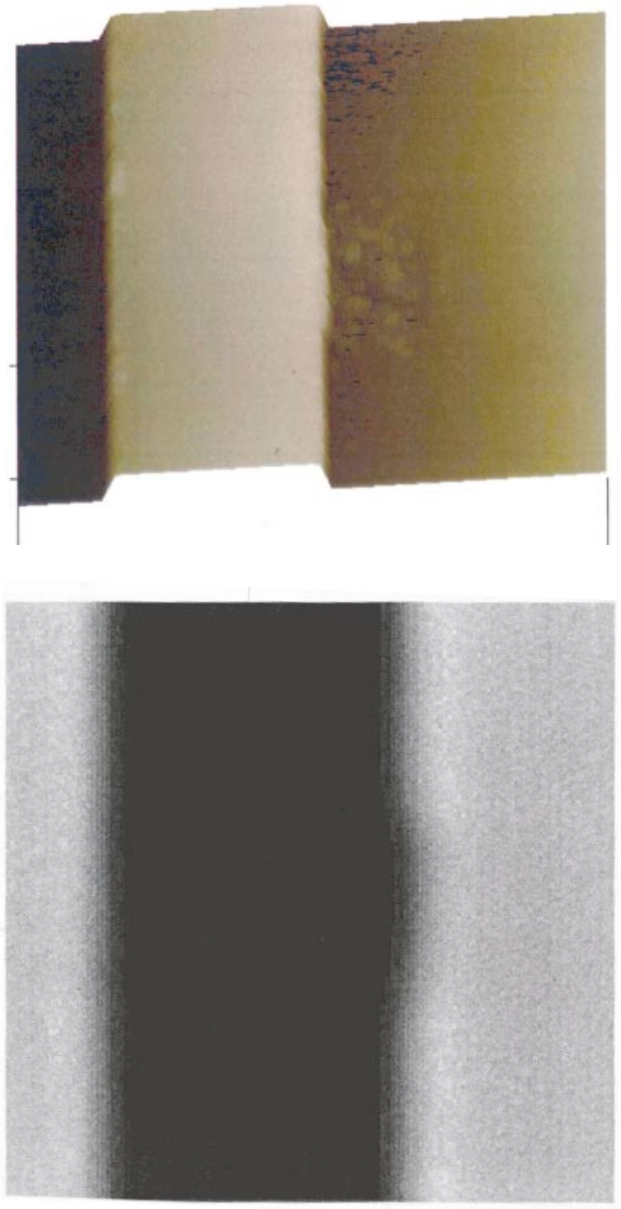

Fig. 6. (A) AFM and (B) AIMS data for a 3 μm edge defect.

clear indicating that the repair does not impact the process tolerances. The edge placement, which amounts to less than 10% of the CD, while not perfect, is acceptable.

AFM and AIMS data from an additional repair are shown in Fig. 6. In this example, a 3 μm square edge protrusion was removed from the right side of the line. Here too, no significant residual material or substrate penetration is evident and the transmission after the repair is excellent.

Conclusion

In this paper we have demonstrated precise near-field ablative removal of thin chrome films for application in photomask repair. The near-field imaging and positioning capability has allowed edge placement accuracies that can not be matched by other optical techniques. The introduction of a femtosecond laser has resolved the outstanding problem of substrate damage and transmission quality after repair. Thus, the incorporation of a femtosecond laser into our near-field optical system provides a unique combination capable of simultaneously addressing the two main challenges of high-resolution photomask repair.

References

Lieberman, K. (1997) Near-field mask repair. *Microlithography World*, Spring 1997.

Lieberman, K., Ignatov, A., Rudman, M., Melnik, I. & Lewis, A. (1999) Near-field optical imaging and patterning of large samples. *Ultramicroscopy*, in press.

Lieberman, K., Terkel, H., Rudman, M., Ignatov, A. & Lewis, A. (1996) High resolution deep UV laser mask repair based on near-field optical technology. *SPIE Proc.* **2793,** 481–488.

Nolte, S., Momma, C., Jacobs, H., Tunnermann, A., Chichkov, B.N., Wellegenhousen, B. & Wellig, H. (1997) Ablation of metals by Ultrashort Pulses. *J. Opt. Soc. Am. B*. **14,** 2716.

Rudman, M., Shchemelinin, A., Lieberman, K. & Lewis, A. (1994) Near-field nanofabrication with pipette guided ArF excimer laser. *SPIE Proc.* **2197**.